

This discussion paper is/has been under review for the journal The Cryosphere (TC).
Please refer to the corresponding final paper in TC if available.

Recent wind driven high sea ice export in the Fram Strait contributes to Arctic sea ice decline

L. H. Smedsrud¹, A. Sirevaag^{2,1}, K. Kloster³, A. Sorteberg^{2,1}, and S. Sandven³

¹Bjerknes Center for Climate Research, Bergen, Norway

²Geophysical Institute, Univ. of Bergen, Norway

³Nansen Environmental and Remote Sensing Centre, Bergen, Norway

Received: 5 April 2011 – Accepted: 18 April 2011 – Published: 5 May 2011

Correspondence to: L. H. Smedsrud (lars.smedsrud@uni.no)

Published by Copernicus Publications on behalf of the European Geosciences Union.

1311

Abstract

Arctic sea ice area decrease has been visible for two decades, and continues at a steady rate. Apart from melting, the southward drift through Fram Strait is the main loss. We present high resolution sea ice drift across 79° N from 2004 to 2010. The ice drift is based on radar satellite data and correspond well with variability in local geostrophic wind. The underlying current contributes with a constant southward speed close to 5 cm s⁻¹, and drives about 33 % of the ice export. We use geostrophic winds derived from reanalysis data to calculate the Fram Strait ice area export back to 1957, finding that the sea ice area export recently is about 25 % larger than during the 1960's. The increase in ice export occurred mostly during winter and is directly connected to higher southward ice drift velocities, due to stronger geostrophic winds. The increase in ice drift is large enough to counteract a decrease in ice concentration of the exported sea ice. Using storm tracking we link changes in geostrophic winds to more intense Nordic Sea low pressure systems. Annual sea ice export likely has a significant influence on the summer sea ice variability and we find low values in the 60's, the late 80's and 90's, and particularly high values during 2005–2008. The study highlight the possible role of variability in ice export as an explanatory factor for understanding the dramatic loss of Arctic sea ice the last decades.

1 Introduction

Arctic sea ice area has decreased since the 1990's (Gloersen and Campbell, 1991). Regardless of the definition of the summer minimum sea ice area (average sea ice extent for September, minimum of daily sea ice area, or the local temporal minimum), the trend is now close to -9 % per decade (Zwally and Gloersen, 2008). Much discussion arose after the minimum September ice cover in 2007 (Stroeve et al., 2007), but the ice area loss has been back on a linear trend recently (Stroeve and Meier, 2010). These linear trends suggest a summer ice free Arctic between 2050 and 2080, comparable

to 1-D models applying increased long wave radiation due to ongoing global warming (Smedsrud et al., 2008). Less predictable future changes are related to changes in cloud cover (Sorteberg et al., 2007) and atmospheric circulation (Overland et al., 2008).

5 For better predictions of future Arctic sea ice evolution we need to understand past changes. The present generation of General Circulation Models generally underestimates the ice loss during the last decades (Stroeve et al., 2007), and future predictions indicate a range from steady state year 2000 conditions, to no summer ice in 2080 (Boe et al., 2009). The Arctic sea ice cover responds to many different types of forcing,
10 but the ice export clearly has direct impact (Björk, 1997), and may have contributed effectively to the observed sea ice thinning (Haas et al. 2008; Kwok, 2009). An increase in the ice export leads to more open water, more solar radiation into the ocean mixed layer, and stronger summer melting (Perovich et al., 2008). The decreasing ice and snow cover has also produced the near-surface temperature 'amplification' and
15 increasing incoming long-wave radiation due to increased moisture fluxes (Screen and Simmonds, 2010), both positive feedback mechanisms.

The destiny of many Arctic sea ice floes is to leave the Arctic Ocean along the eastern coast of Greenland (Fig. 1). As first documented by the passive drift of the ship Fram (Nansen, 1906), a large area of sea ice is lost annually from the Arctic Ocean to
20 the Greenland Sea through what was later termed the Fram Strait. Around 10 % of the Arctic sea ice cover is exported annually, and estimates have improved over the last decade (Vinje, 2001; Kwok et al., 2004; Kwok, 2009).

Trends in Fram Strait sea ice export have previously not been found, but within the Arctic Ocean sea ice drift speed has increased based on ice station and bouy data
25 since the 1950's (Hakkinen et al., 2008). Increased speed has also been detected in the Fram Strait after 1979. Section 3 presents southward ice velocities across 79° N in the Fram strait based on high accuracy Synthetic Aperture Radar (SAR) data onwards from 2004. High correlations between the ice drift and geostrophic winds from atmospheric reanalysis data allow for calculations of the sea ice export back to the 1950's.

1313

Earlier estimates of sea ice export and speed have mostly been based on passive satellite data with coarser spatial resolution (Rampal et al. 2009; Kwok, 2009). We find that the ice export has been high in recent years, and discuss likely consequences and causes of this high export in Sect. 4. We conclude (Sect. 5) that the recent high
5 ice export must have influenced both the September minimum ice cover of the last few years, and the general thinning of Arctic sea ice.

2 Data and methods

Sea ice area export was calculated from sea ice motion and ice concentration profiles along 79° N. Onwards from August 2004 ice drift vectors were calculated from pairs of
10 Envisat ASAR WideSwath images captured 3 days apart with uninterrupted year-round coverage. Images were averaged to 300 m/pixel spatial resolution, corresponding to a speckle noise well below 0.3 dB.

The manually recognized persistent ice features were gridded to 2 km accuracy and the corresponding displacement vectors that cross 79N were linearly interpolated to
15 bins (1° longitude, each 21 km) from 15° W to 5° E. For most 3-day image pairs, displacement vectors with accuracy about 10 % were found with a spacing of 30–50 km, including interpolation/extrapolation in the shear/ice edge zones. As the vectors can be assumed non-biased, cumulative motion over longer periods will have improved accuracy. We based ice concentration on Norsex algorithms used respectively on DMSP
20 F13 SSMI and AQUA AMSR-E brightness temperature data, giving the combined ice-area flux along 79° N, between 2004 and 2010 (Kloster and Sandven, 2011). Our mean of approx. 4500 observations of sea ice velocity along 79° N was 12.0 cm s⁻¹ southward (s.d. ± 8.7) with a small westward component (4.3 cm s⁻¹, s.d. ± 5.7). Monthly mean area export uncertainties were estimated to 5 %.

25 We used sea level pressure difference from 80° N in the NCEP/NCAR reanalysis products (Kalnay et al., 1996) from 1957-present. As air pressure measurements were not synchronised globally before the International Geophysical Year in 1957 we have

1314

found eastward, with a gradual increase in speed further east. On the whole western side ice concentration is close to 100 % during winter, but ice drift is low (Fig. 1). On the eastern end ice export is limited by zero concentration, varying between 5° W and 5° E. Ice velocity generally increases eastward, while sea ice concentration decreases, creating a peak in ice area export near 5° W (Figs. 1 and 6). The yearly cycle in area export is pronounced. Figure 3 shows that the major export occurs between October and April, and that there is close to zero export in July and August.

We found no evidence for a seasonal cycle in the East Greenland Current. Foldvik et al. (1988) analysed one year long time series from three moorings along 79° N between 6 and 2° W and found large mesoscale eddies meandering southwards, but no obvious seasonal variability. Southward flow was in the range 6.2 to 9.5 cm s⁻¹, decreasing east of 2° W. Our results with a mean southward flow throughout the year between 2004 and 2010 is thus consistent with earlier studies. From Eq. (1) the mean current is estimated to 4.95 cm s⁻¹, also consistent with current measurements from 79° N 5° W (Widell et al., 2003) between 1996 and 2000. Figure 4 shows that since 2004 the ice export approaches zero for two to three summer months every year. This is caused by winds from the south (negative cross straight pressure gradient) opposing the steady southwards flowing current below the sea ice.

In the case of no wind forcing, or zero cross straight pressure difference, there is still a steady export of sea ice. Our contribution from this steady current is an ice area flux of 24 562 km² pr month, This means that the East Greenland Current has driven ~33 % of the ice export since 2004. Compared to previous estimates at 81° N (Kwok, 2009) our pressure dependency is 19 % larger, while our constant term (Eq. 3) is 12 % lower. Ice speed correlates better with geostrophic wind than ice area export ($r_{\text{speed}} > r_{\text{area}}$), probably because geostrophic wind influences ice concentration to a small degree.

3.3 SAR – AMSR Comparison

We compared our SAR based ice speed data directly with ice speed estimates based on Advanced Multichannel Scanning Radiometer (AMSR) (Ezraty et al., 2010). AMSR

1317

data is available (from October through April), and we therefore used 3-day periods for this period of the year in our comparison. Generally no ice speed estimates are available from passive satellites during summer, but it is the winter months that have the largest ice area flux (Fig. 3). For each 3-day period from February 2004 to April 2010 available AMSR ice drift vectors crossing 79° N were averaged in the same longitude bins as for the SAR data. Figure 5 compares the northward velocity components for time periods and longitude intervals where velocity data exists in both data sets. AMSR data exist for overall 34 % of the total number of longitude bins. The linear fit in Fig. 5 shows that there is good correspondence in the mean between SAR and AMSR derived drift vectors. The considerable spread may be caused by several factors, but we hold these to be the most important: (1) the vectors time-of-day may differ, (2) AMSR has many non-zero drifts in the fast ice (at zero SAR speed), and (3) AMSR often under-estimates large speeds (at high SAR speed). However, on the average the figure gives a good reassurance in the two data sets, and indicates that the magnitude of the northward velocity estimates over the 6 years are close to reality.

Figure 6 shows the temporal coverage of the AMSR data in each longitude bin. The AMSR data has good coverage in the westernmost longitude bins, but it is dropping below 10 % east of 3° W. The relative contribution to the total ice area flux for each longitude bin, derived from the SAR ice drift velocities, is also included in Fig. 6. In the bins between 15 and 10° W AMSR coverage is above 50 %, but these bins carry a very small part of the ice export. The average AMSR coverage in the longitude bins which accounted for more than 90 % of the total ice area flux (Fig. 6, 11 to 0° W), was as low as 29 %. The low temporal coverage of AMSR data in the longitude range which house most of the ice export during the winter season, is a likely explanation for why the variability demonstrated by our SAR based ice area fluxes have not been detected in other data sets.

- Sorteberg, A. and Walsh, J. E.: Seasonal cyclone variability at 70 degrees N and its impact on moisture transport into the Arctic, *Tellus*, 60, 570–586, doi:10.1111/j.1600-0870.2008.00314.x, 2008. 1315, 1320
- Sorteberg, A., Kattsov, V., Walsh, J., and Pavlova, T.: The Arctic surface energy budget as simulated with the IPCC AR4 AOGCMs, *Clim. Dynam.*, 29, 131–156, doi:10.1007/s00382-006-0222-9, 2007. 1313, 1315
- Stroeve, J. and Meier, W.: Sea Ice Trends and Climatologies from SMMR and SSM/I, http://nsidc.org/data/seaice/data_summaries.html, 2010. 1312, 1322
- Stroeve, J., Holland, M., Meier, W., Scambos, T., and Serreze, M.: Arctic sea ice decline: Faster than forecast, *Geophys. Res. Lett.*, 34, doi:10.1029/2007GL029703, 2007. 1312, 1313
- Thorndike, A. and Colony, R.: Sea Ice Motion in Response to Geostrophic Winds, *J. Geophys. Res.*, 87, 5845–5852, 1982. 1315, 1316
- Tsukernik, M., Deser, C., Alexander, M., and Tomas, R.: Atmospheric forcing of Fram Strait sea ice export: a closer look, *Clim. Dynam.*, doi:10.1007/s00382-009-0647-z, 2009. 1315
- Uppala, S. M., Kallberg, P. W., Simmons, A. J., Andrae, U., Bechtold, V. D., Fiorino, M., Gibson, J. K., Haseler, J., Hernandez, A., Kelly, G. A., Li, X., Onogi, K., Saarinen, S., Sokka, N., Allan, R. P., Andersson, E., Arpe, K., Balmaseda, M. A., Beljaars, A. C. M., Van De Berg, L., Bidlot, J., Bormann, N., Caires, S., Chevallier, F., Dethof, A., Dragosavac, M., Fisher, M., Fuentes, M., Hagemann, S., Holm, E., Hoskins, B. J., Isaksen, I., Janssen, P. A. E. M., Jenne, R., McNally, A. P., Mahfouf, J. F., Morcrette, J. J., Rayner, N. A., Saunders, R. W., Simon, P., Sterl, A., Trenberth, K. E., Untch, A., Vasiljevic, D., Viterbo, P., and Woollen, J.: The ERA-40 re-analysis, *Q. J. Roy. Meteorol. Soc.*, 131, 2961–3012, 2005. 1316, 1320
- Vinje, T.: Fram strait ice fluxes and atmospheric circulation: 1950–2000, *J. Climate*, 14, 3508–3517, 2001. 1313, 1315, 1320, 1321, 1322, 1324
- Widell, K., Østerhus, S., and Gammelsrød, T.: Sea ice velocity in the Fram Strait monitored by moored instruments, *Geophys. Res. Lett.*, 30(19), 1982, doi:10.1029/2003GL018119, 2003. 1315, 1317, 1320, 1322
- Winsor, P.: Arctic Sea Ice Thickness Remained Constant During the 1990s, *Geophys. Res. Lett.*, 28, 1039–1041, 2001. 1321
- Zwally, H. J. and Gloersen, P.: Arctic sea ice surviving the summer melt: interannual variability and decreasing trend, *J. Glaciol.*, 54, 279–296, 2008. 1312, 1323

1327

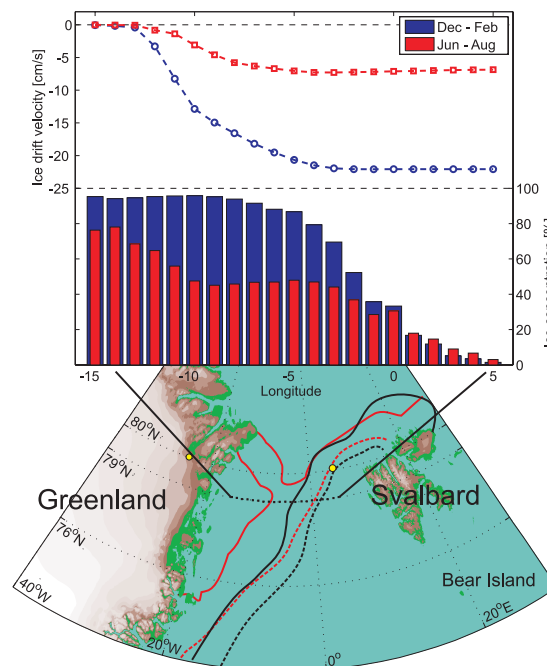


Fig. 1. The Fram Strait between Greenland and Svalbard and mean sea ice properties for 2004–2010. Ice cover for summer (red, June through August) and winter (black, December through February) as solid (50 %) and dashed lines (15 %). Above: southward ice drift across 79° N from August 2004 to July 2010 in 1° bins based on SAR imagery, and ice concentration from SSMI and AMSR data. The ice area export is found by multiplying the ice drift and ice concentrations. Yellow circles show locations for surface pressure data used.

1328

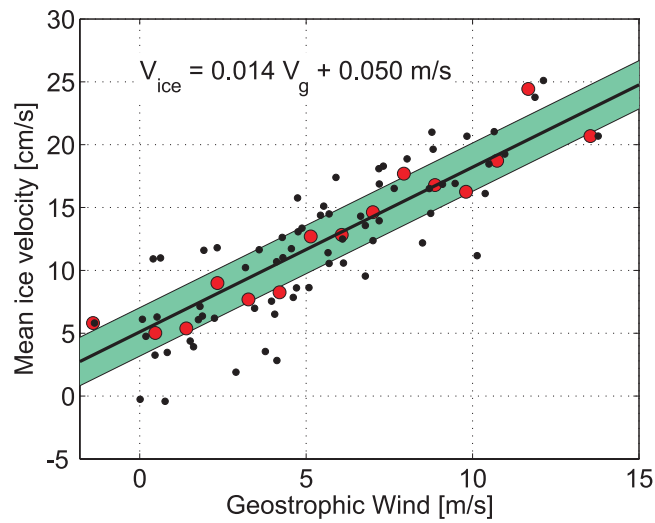


Fig. 2. Linear fit between Fram Strait southward ice velocity and geostrophic wind. Monthly averages are shown as black dots and are averaged along 79° N. Binned values are shown as red circles. The shaded area is the standard error estimate of the linear fit.

1329

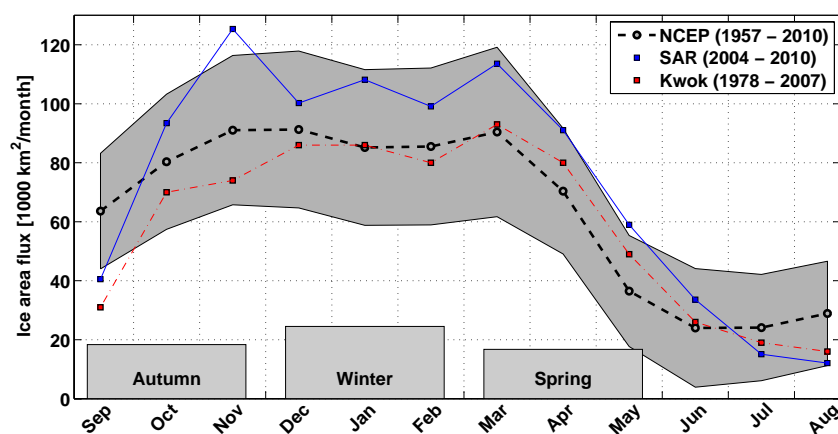


Fig. 3. Monthly mean Fram Strait sea ice area export during the year. Values from Kwok (2009) are added for comparison. Standard deviations of the NCEP values are shaded in grey. Changes in seasonal monthly ice export (1957–2010) are plotted at the bottom.

1330

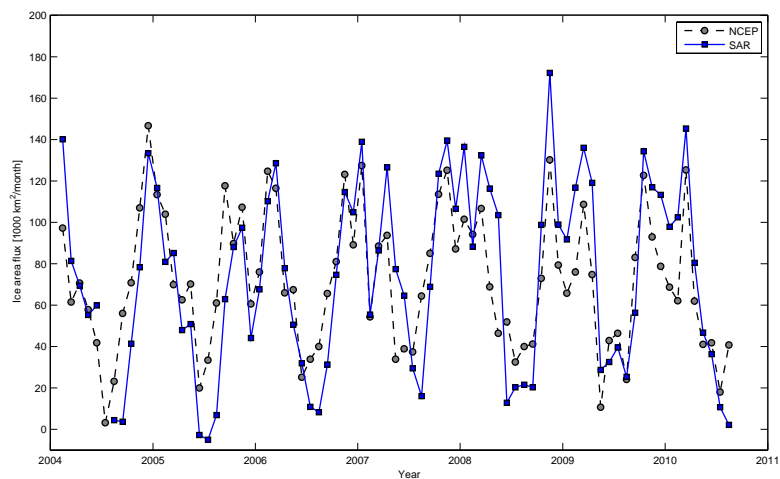


Fig. 4. Monthly ice area export values based on SAR velocity compared to the NCEP pressure difference formula (Eq. 3.)

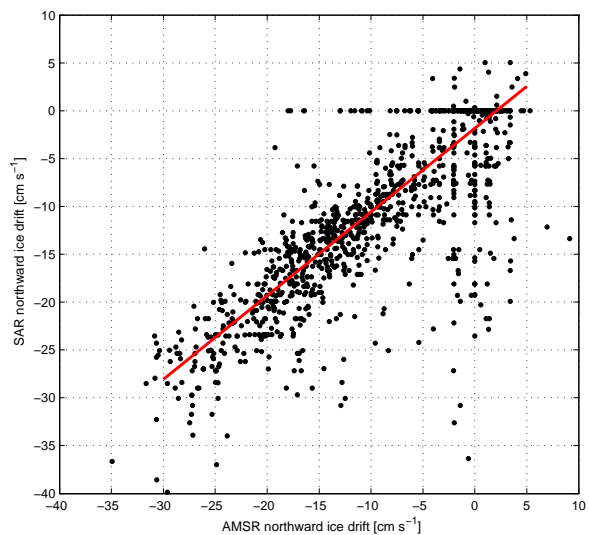


Fig. 5. Comparison between southward ice drift speeds across 79° N in the Fram Strait from SAR and AMSR data. The data covers winters (October through April) between 2004 and 2010. Individual values are estimated 3-days drift velocities for a given longitude bin. Red line is a linear fit.

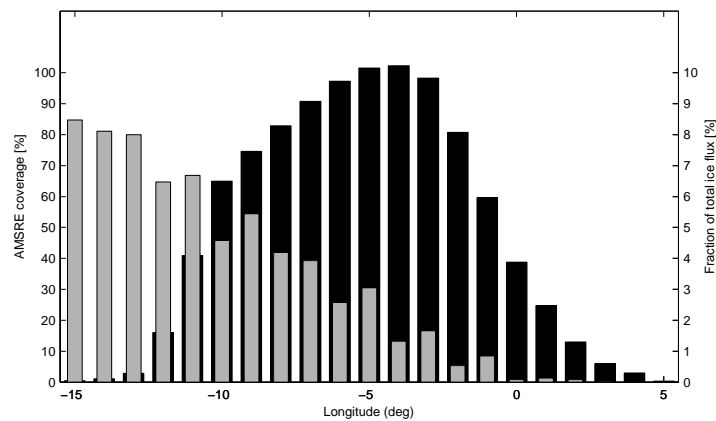


Fig. 6. Coverage of AMSR ice speed data along 79° N in the Fram Strait, contrasted with our new SAR based ice area export estimates. The period covered is October through April from 2004 to 2010. A 50 % value (grey bars, left axis) means that the actual longitude bin has AMSR ice drift velocity estimates for 50 % of the time. Black bars shows the contribution to the total ice flux for the individual longitude bins (right axis), calculated from the SAR ice drift velocities for the same period. The SAR data coverage is 100% for all bins, i.e. we have an ice velocity measurement for every bin every 3 days.

1333

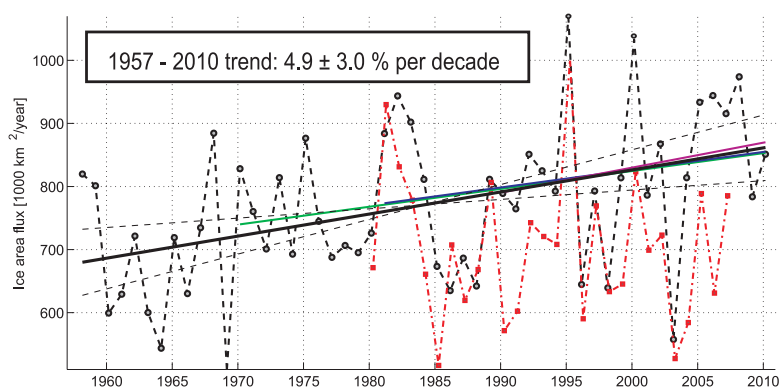


Fig. 7. Annual mean Fram Strait sea ice area export values as driven by NCEP surface pressure difference. Values are averages for 1 September through 31 August. Dashed lines indicate the 95 % confidence interval of the trend. Linear trends are added onwards from 1970, 1980 and 1990 (different colours). Values from Kwok (2009) are added for comparison.

1334